

INNOVATIVE SYNTHESIZE OF ZrO₂ NANOMATERIAL USING BIODEGRADABLE DRAGON FRUIT PEEL EXTRACTS AND ITS PHOTOCATALYTIC ACTIVITY AGAINST METHYL ORANGE BY UV RADIATION

Kistan^{1✉}, V. Kanchana², S. Mohan³ and M. Chitra⁴

¹Department of Chemistry, Panimalar Engineering College, Chennai-600123,
(Tamil Nadu) India

²Department of Chemistry, Sree Sastha Institute of Engineering and Technology,
Chennai-600123, (Tamil Nadu) India

³Department of Chemistry, Rajalakshmi Engineering College, Chennai-602105,
(Tamil Nadu) India

⁴Department of Chemistry, Chellammal Women's College, Chennai-600032,
(Tamil Nadu) India

✉Corresponding Author: vishmikirish@gmail.com

ABSTRACT

The motivation behind this study is to stress the worth of green amalgamation in the development of nanomaterials. Regarding this declaration, we said that we have examined the morphological, optical, underlying, and photocatalytic color debasement exercises of the incorporated ZrO₂ nanoparticles as well as their biosynthesis by means of a response intervened by mythical serpent organic product bloom separate. UV-noticeable spectroscopy was utilized to identify a huge absorbance top at 360 nm. The utilization of SEM affirmed that the nanoparticles, which had a typical size of 17.5 nm, were circular in shape. The nanoparticles' zirconium (70.88%) and oxygen (29.12%) contents were checked utilizing energy-dispersive X-beam examination. The nanoparticles' X-beam powder diffraction (XRD) spectra demonstrated their crystallinity. While the information from HR-TEM shows particles that are 33.75 nm in size. When the photocatalytic movement of ZrO₂ NPs was researched, Methyl Orange showed 54.2 % debasement following 120 minutes of UV openness and 68.50 % corruption following an hour and a half of UV openness, individually. This fresh-out of the plastic bio-ZrO₂ nanoparticle was utilized to study the photocatalytic breakdown of methyl orange when presented with apparent light. The cationic color was separated by the engineered bio-ZrO₂ shortly with 91.8 % corruption ability.

Keywords: Nano ZrO₂, Dragon Fruit Peel, Photocatalytic Activity, Methyl Orange.

RASAYANJ. Chem., Vol. 17, No.1, 2024

INTRODUCTION

The end or expulsion of colors from polluted streams has been endeavored to utilize various synthetic and natural systems, including electrochemical strategies, compound medicines, initiated carbon-helped adsorption, and ozone treatment, among others. The upsides of involving NPs in the photocatalysis cycle (high surface-volume proportion, high surface energy, prevalent qualities than materials on a perceptible scale, and so forth.) have been concentrated as of late. Aqueous, solvothermal, gel sol, and compound fume precipitation, radiation substance decrease, sonochemical strategies, ultrasonic light, and microwave-helped blend are a couple of the most involved methods for making NPs advance an electron from the valence band (BV) over into the conduction band (CB) and make an electron-opening pair (e⁻h⁺), the photocatalysis cycle includes the excitation of an electron¹⁻⁴, which is achieved by the retention of light with an energy equivalent to or more prominent than the band hole of the photocatalysts. The negative electrons in the BC lessen oxygen to make superoxide revolutionaries (O₂²⁻), and the positive hole made in the BV oxidizes close by water particles to deliver hydroxyl extremists (OH•). The two extremists are strong oxidizing substances that assist impurities in water with corrupting. Water pollution is mostly caused by the overuse of agrochemicals (fertilizers and pesticides), pharmaceuticals and

personal care products, domestic waste, and industrial waste discharges, such as heavy metals and organic dyes. An estimated 7.0 105 tons of synthetic dyes are generated annually, of which 2.0 105 tonnes are lost to the environment (lakes, rivers, seas, and oceans) as a result of the textile industry's inefficient dying process, causing significant pollution and health problems. Most organic dyes cause burns, cancer, dermatitis, respiratory and digestive problems, as well as mental difficulties, among other problems.⁵⁻¹⁰ This unique technique of biosynthesis has enabled results with elements from nature but is still equivalent to chemical NP synthesis approaches. Plant extracts have received an abundant deal of consideration for green synthesis because of their non-pathogenicity and the tightly regulated assembly of biomolecules synthesized during biosynthesis. Additionally, biomolecules contained in plant extracts such as polyphenols and amines, which can act as metal salt reducers, can lower aqueous solutions.¹¹⁻¹³ An excellent replacement is plant-mediated synthesizing, which is also user-friendly and environmentally responsible. These plant-mediated metal oxide nanoparticles have extensive uses in biomedicine, photocatalysis, antibacterial therapy, sensors, and antioxidants.¹⁴ Many nations around the world see a considerable impact from the textile sector on their economies. These industries generate high or low-color wastes depending on the degree of fixing of the dyestuffs on the substrates, which differs with the nature of the materials, the expected intensity of color, and the application technique.¹⁵ Given the state of the environment today, it is widely acknowledged that human activity and scientific advancement are to blame for the loss of drinking water's properties. New techniques and materials are being developed by researchers that can be used to turn wastewater into a resource for everyday usage.¹⁶

An advanced technique for environmental management is the use of zirconium oxide nanoparticles in the dye removal business. Thus, the focus of this research is on creating more ecologically friendly Nanocomposites from biopolymers for widespread use in dye adsorption, fuel cells, sensors, and dentistry domains.¹⁷ The study is distinctive in that it explains the production of zirconium oxide nanoparticles using only environmentally friendly methods, with the removal of Methyl Orange dye being one of its uses. As a result, our study will advance the field of dye degradation using synthetic ZrO₂ nanoparticles that are safe for the environment.¹⁸⁻²⁰ On the other hand, nothing is known at this time about the application of this dragon fruit flower extract in ZrO₂ nanoparticles. In this work, we report a green chemical process for preparing ZrO₂ nanoparticles (NPs) from dragon fruit flowers. As a result, the suggested work implies that producing zirconium oxide nanoparticles through green synthesis is a highly cost-effective and environmentally responsible method. The BFE-ZrO₂ nanoparticles' photo-degradation potential was examined. It is also predicted that broad implementation of this approach will contribute to the improvement of contemporary, eco-friendly elements for future research purposes.

The green ZrO₂ nanoparticles that were produced with the help of extract from dragon fruit flower show potential for use in wastewater applications because they are efficient photocatalysts for the detection and removal of organic environmental pollutants in water bodies close to the textile, dye, and tannery industries, among others.

EXPERIMENTAL

Materials

Sigma-Aldrich was the source of all other chemicals and reagents, including the 99.4 % pure methyl orange-red dye. All of the glassware was completely rinsed with de-ionized water and acid-washed before use. Double distilled water was used for each experiment.

Collection of Dragon Fruits and Peel

During the post-monsoon season (March 2023) in Chennai, Tamil Nadu, South Eastern India, dragon fruit peels were purchased from local vegetable markets.

Preparation of Dragon Fruits Peel Extract

To extract the pulp, the dragon fruits and peel were cut open (Fig.-1). At -50 °C and 0.040 mbar, the pulp was freeze-dried for 48 to 72 hours using a Christ Freeze Dryer Alpha 1-4LD Plus. Using an MRC Knife Mill Cup, the material was ground into a powder and stored at -80 °C until required.

ZrO₂ Nanoparticle Synthesis Employing Extract from the Peel of Dragon Fruits

Ten milliliters of peel extract from dragon fruits were treated separately with Separate 0.1M, 0.3M, and 0.5 M Zirconyl nitrate solutions were added to 10 ml of Dragon Fruit peel extract, and the mixture was agitated for three hours at 80°C. To further purify it, it was centrifuged for 30 minutes at 5000 rpm. Deionized water was then used on a regular basis to clean it. After that, it was kept for two hours at 120°C in a hot air oven.



Fig.-1: Dragon Fruits and Peel

The 500°C calcination process took four hours to produce the dark brown powder. The 0.3M and 0.5M preparations were being made using the same process, respectively. The reaction mixture's color changed from light brown to dark brown, indicating that BFE-ZrO₂ NPs had formed. The explanation for this is that phenolic chemicals, which are found in CFE, reduce Zr²⁺ ions to Zr⁰. Extracts from flowers have been found to function as both a capping agent and a reducing agent for the metal nanoparticles.

Characterization

All powdered X-ray diffraction (XRD) patterns were obtained using an Analytical (X'Pert PRO) diffractometer equipped with a Cu-K radiation source (= 0.1541 nm). The ELICO SL-159 spectrophotometer was used to measure the UV-Vis absorption spectra. Using a 5DX FT-IR spectrometer (spectral resolution 2 cm⁻¹), the FT-IR spectra of a dry potassium bromide pellet at room temperature were captured in the 4000-400 cm⁻¹ region. The morphology of the material was investigated using the field emission-scanning electron microscopy (CARELZEISS) model EV018. All TEM images were taken at room temperature (RT, 298K) using an electron microscope (JEOL SM-7600 F, Japan) equipped with a field-emission gun at an acceleration voltage of 200 KV. The maximum number of nanoparticles is determined using dynamic light scattering (DLS) experiments.

Photocatalytic Activity

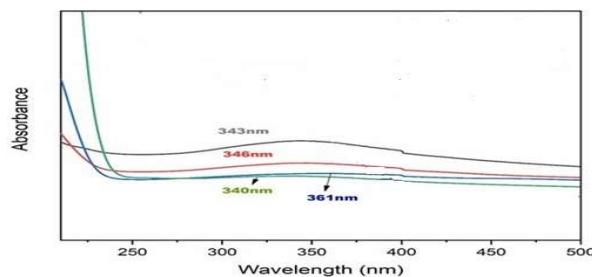
Methyl Orange dye was degraded under the effect of D-2 Lamp and Tungsten halogen lamp (W Lamp power is: AC 220V / 50 Hz) to determine the photocatalytic activity of BFE-ZrO₂ nanoparticles. Ten milliliters (ml) of a dye solution (0.05 g) were added to 50 mg of BFE-ZrO₂ nanoparticles. The photo reaction vessel and UV source were placed 10 cm apart. After turning on the lights and recording the readings, the suspension was agitated for 30 minutes in a dark medium.²¹⁻²⁴ The concentrations of various aqueous suspensions (Methyl Orange) in each sample were determined using comparable techniques.

$$\text{Effect of DPPH scavenging (\% inhibition)} = \frac{[(\text{control absorbance} - \text{reaction mixture absorbance}) / \text{control absorbance}] \times 100}{}$$

RESULTS AND DISCUSSION

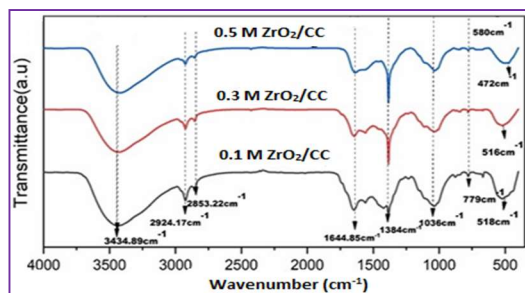
UV Visible Spectroscopy

The utilization of UV-visible spectroscopy to evaluate the optical characteristics of as-prepared BFE-ZrO₂ nanoparticles, as illustrated in Fig.-1. The broad maximum absorbance of the broccoli flower extract in the UV-visible spectrum was found to be 361 nm; the other absorbance is 343 nm and 346 nm. Consequently, we were able to verify that ZrO₂ nanoparticles were made via plant extraction.

Fig.-1: UV-visible Spectrum for BFE-ZrO₂ Nanoparticle

Fourier Transform Infra-Red Spectroscopy (FT-IR)

The functional groups for ZrO₂ production (0.1M, 0.3M, and 0.5M) in the CC flower extract were found using FTIR analysis. The absorption bands for the ZrO₂ nanoparticles are displayed in Fig.-2 at 3434, 2924, 2853, 1644, 1384, 1036, 779, and 472 cm⁻¹. We conclude that the compound contains proteins and amino acids based on the large absorption peak at 3434 cm⁻¹, which may have been caused by the presence of phenolic compounds with an O-H bond stretching, and the peak at 1644 cm⁻¹, which is caused by an amine N-H bending vibration bond.³⁰ The 1384 cm⁻¹ and 1030 cm⁻¹ peaks, respectively, are correlated with the aromatic vibrations' O-H and C-O stretching groups. The phenolic groups and the alcoholic group C-N Stretching vibration are represented by the strong peaks that can be seen at 1380 cm⁻¹ and 1035 cm⁻¹, respectively. Zr-O vibrations were observed in the peaks of the absorption bands at 470-778 cm⁻¹.

Fig.-2: FT-IR Spectrum for BFE-ZrO₂ Nanoparticle

X-ray Diffraction Analysis

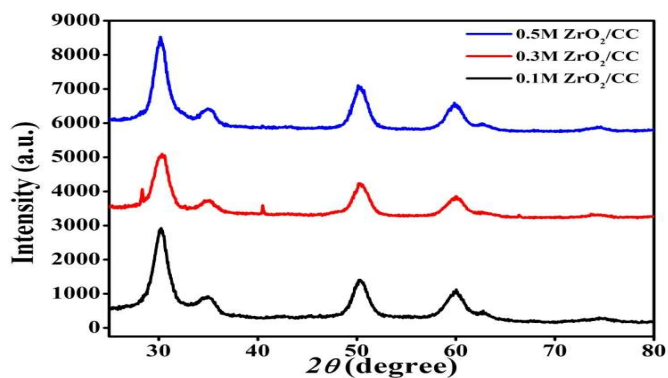
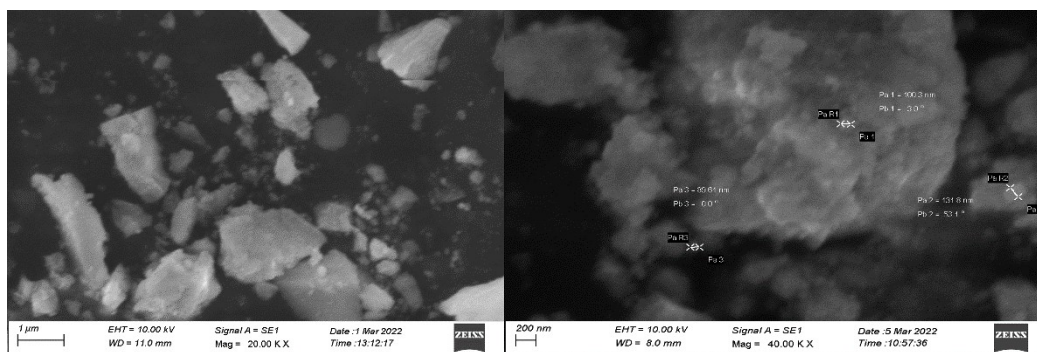
Utilization of X-ray diffraction to verify the phase of the DFE-ZrO₂ nanoparticles (0.1M, 0.3M, and 0.5M). The peaks at 2 values of 30.18, 35.08, 40.51, 50.30, and 59.88, respectively, represented the crystal planes (111), (200), (211), (220), (131), and (131). The Joint Committee on Powder Diffraction (JCPDS Card No. 79-1766), which was used to discuss similar X-ray diffraction, has set standards for the tetragonal phase, which this peak demonstrates to be in compliance with. The zirconium oxide nanoparticles were shown to be well-crystalline by the strong, highest, narrowest peaks (111) (Fig.-3). The ZrO₂ nanoparticle's average particle size was determined using the Debye-Scherer formula:

$$D = \frac{0.9\lambda}{2\beta\cos\theta}$$

Where β is the peak's Full Width at Half Maximum (FWHM), D is the crystal size, and λ is the wavelength of the Cu-K α radiation. The average particle size of ZrO₂ nanoparticles was 17.6 nm.

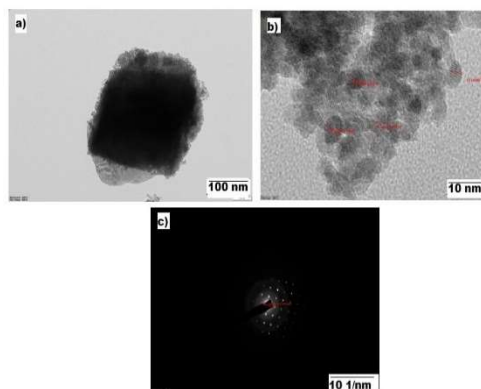
Scanning Electron Microscope (SEM)

SEM analysis revealed that the green synthesized ZrO₂ nanoparticles were spherical and triangular in shape (Fig.-4). The synthesized DFE-ZrO₂ nanoparticle was analyzed using Energy energy-dispersive X-ray to determine its elemental composition. Of the elements, zirconium makes up 70.88% and oxygen makes up 29.12%.

Fig.-3: XRD Spectrum for BFE -ZrO₂ NanoparticleFig.-4: SEM images of BFE- ZrO₂ Nanoparticle

Transmission Electron Microscopy (TEM) with SAED

The size formation and surface features of green synthesized BFE-ZrO₂ nanoparticles demonstrated their homogeneity and nanoscale. Most of these BFE-ZrO₂ NPs have a cubic shape and are between 5 and 100 nm in size. The SAED analysis of BFE-ZrO₂ nanoparticles revealed a crystalline structure with a length of $6.174 \times 10^{-1} \text{ nm}$, as shown in the ring-like pattern shown in Fig.-(5a, & 5b).

Fig.-5: High-Resolution TEM Images (5a and 5b) for BFE-ZrO₂ Nanoparticle and the Selected Area Electron Diffraction(SAED) Were Shown in Fig.-5c

Dynamic Light Scattering (DLS)

The DLS method is recommended for the analysis of particles sized between 93.6 nm and 103.5 nm. The average particle size of the biosynthesized BFE-ZrO₂ nanoparticles (0.1M, 0.3M, and 0.5M) was determined to be 93.7 nm. ZrO₂ nanoparticles with diameter values of 93.6, 84.2, and 103.5 were produced using dragon fruit peel extract at concentrations of 0.1M, 0.3M, and 0.5M. Some of the factors

that affect the assessment of particle size are the size of surface structures, the size of the particle core, and the concentration of the particles. Figure-6 displays the findings of the particle size measurements.

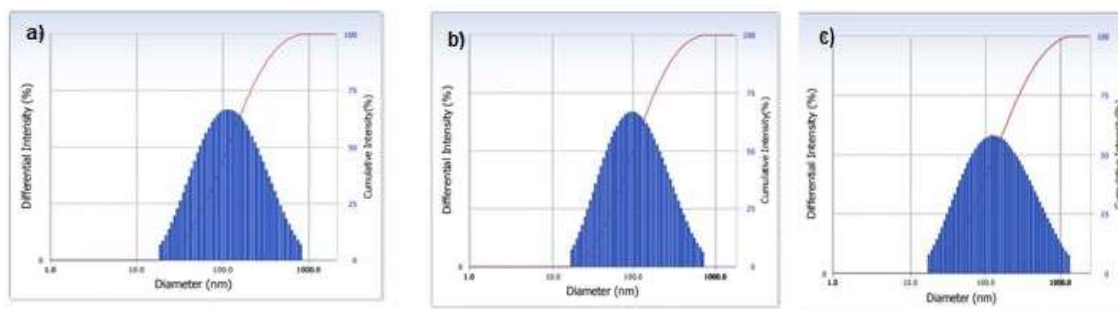


Fig.-6: DLS Analysis for BFE -ZrO₂ Nanoparticle

Photocatalytic Studies

BFE-ZrO₂ nanoparticles' photocatalytic activity was employed to study the methylene red dye's degradation in an aqueous solution. ZrO₂ nanoparticles were produced using various concentrated solutions (10 g/ml, 50 g/ml, 100 g/ml, 250 g/ml, and 500 g/ml). The suspensions were magnetically stirred for half an hour in the dark prior to being exposed to radiation. After that, the photoreaction vessel was exposed to UV radiation in a typical setting. The methylene red absorption spectra over time are shown in Fig.-8. (0, 30, 60, 90, 120 and 150 minutes). The unique absorption peak of the MR at 664 nm rapidly decreases after the first hour, and the UV exposure gradually decreases over the next few hours (up to four hours). An illustration of the photo-removal efficiency of the BFE-ZrO₂ nanoparticles is shown in Fig.-7. The highest degradation efficiency is seen at 500 g/ml when comparing all concentrations. At 0 30 60 90 and 120 minutes under UV irradiation, respectively, the percentage degradation of methyl orange was 79.58%, 76.92%, 72.26%, 65.26%, 51.10%, and 17.66%.

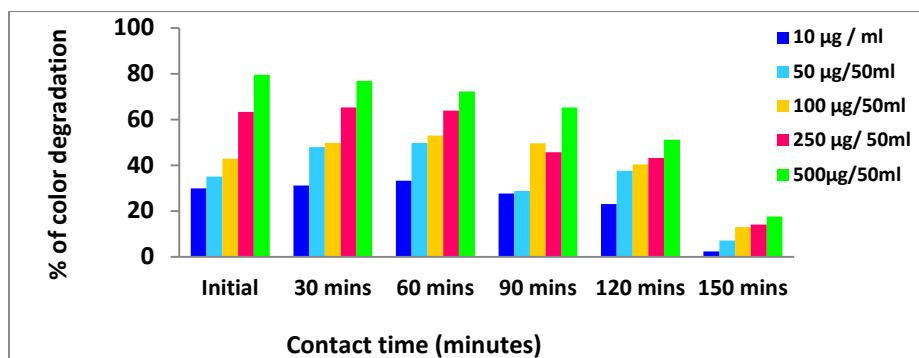


Fig.-7: Photocatalytic Activity of DFE -ZrO₂ Nanoparticles

Table-1: Photo-Catalytic Efficiency of ZrO₂ Nanomaterial's

S. No.	Time interval (Minutes)	% of Test sample concentration (mg/ml)					
		Control	10 µg / ml	50 µg/50ml	100 µg/50ml	250 µg/ 50ml	500 µg/50ml
1.	Initial	100	29.90	35.02	42.86	63.28	79.58
2.	30	100	31.20	47.91	49.76	65.22	76.92
3.	60	100	33.22	49.80	52.92	63.80	72.26
4.	90	100	27.62	28.74	49.62	45.68	65.24
5.	120	100	23.10	37.62	40.41	43.20	51.12
6.	150	100	2.32	7.08	12.96	14.12	17.64

The percentage of photo-removal efficiency was calculated using the formula given below:

$$\text{Percentage Photo-degradation} = C_0 - C/C_0 \times 100$$

Where C_0 is the dye's initial concentration and C is the dye's final concentration following photo-irradiation. Consequently, dye degradation occurs when ZrO_2 is present. By measuring a drop in peak intensity using spectrophotometry, it is possible to confirm the presence of a nanoparticle visually.²⁵⁻²⁸

CONCLUSION

The method used to create the CC-zirconium oxide nanoparticles is rapid, secure, and economical. The UV-visible spectrum showed absorbance at 248 nm. ZrO_2 nanoparticles' FT-IR spectra showed a range of functional groups. The average particle size of 63 nm was also confirmed by DLS studies. Using SEM analysis, the size of the ZrO_2 nanoparticles was determined to be in the range of 72.5 nm. The elemental composition was analyzed using the EDAX spectroscopy. XRD analysis verified the trigonal shape and sharp maximum peak of ZrO_2 nanoparticles at the (111) plane, thereby confirming their crystallinity. It was found that the average crystalline size was 5.58 nm. The particle sizes, as determined by High Resolution-TEM analysis, were 5.5 nm, 5.7 nm, and 6.3 nm. The length of the SAED pattern was 6.18 nm. The photocatalytic activity of ZrO_2 was studied at a concentration of 90%. When exposed to ultraviolet light, the synthesized DFE- ZrO_2 nanoparticle highly photocatalytically breaks down the Methyl Orange dye. It is therefore quite helpful in resolving our environmental issues. Thus, these Nano composites successfully inhibited the DPPH assay. These findings imply that photocatalytic and anti-oxidation processes may benefit from the use of the environmentally produced ZrO_2 nanoparticle.

ACKNOWLEDGEMENTS

The authors are appreciative of the help and vital research facilities they received from Panimalar Engineering College (Autonomous) in Chennai, India.

CONFLICT OF INTERESTS

There is no conflict of interest, according to the authors.

AUTHOR CONTRIBUTIONS

All the authors contributed significantly to this manuscript, participated in reviewing/editing, and approved the final draft for publication. The research profile of the authors can be verified from their ORCID IDs, given below:

A. Kistan  <https://orcid.org/0000-0003-1334-4331>

V. Kanchana  <https://orcid.org/0000-0003-3528-5491>

S. Mohan  <https://orcid.org/0000-0001-6538-3055>

M. Chitra  <https://orcid.org/0009-0005-3769-1022>

Open Access: This article is distributed under the terms of the Creative Commons Attribution 4.0 International License (<http://creativecommons.org/licenses/by/4.0/>), which permits unrestricted use, distribution, and reproduction in any medium, provided you give appropriate credit to the original author(s) and the source, provide a link to the Creative Commons license, and indicate if changes were made.

REFERENCES

1. H.A. Jasim, L. Nahar, M.A. Jasim, S.A. Moore, K.J. Ritchie and S.D. Sarker, *Biomolecules*, **11**(8), 1203 (2021), <https://doi.org/10.3390/biom11081203>
2. H.M. Shinde, S. V. Kite, B. S. Shirke, and K. M. Garadkar, *Journal of Materials Science: Materials in Electronics*, **32**(11), 14235 (2021), <http://doi.org/10.1007/s10854-021-05983-7>
3. S. Puiaç, X.H. Sem, A. Negrea and M. Rhen, *International Journal of Antimicrobial Agents*, **38**, 409 (2011), <https://doi.org/10.1016/j.ijantimicag.2011.06.009>
4. Chelliah, Parvathiraja, Saikh Mohammad Wabaidur, Hari Prapan Sharma, Hasan Sh Majdi, Drai Ahmed Smaït, Mohammed Ayyed Najm, Amjad Iqbal, and Wen-Cheng Lai, *Separations*, **10**(3), 156(2023), <https://doi.org/10.3390/separations10030156>
5. M. Chitra, A. Kistan, V. Kanchana. and A. Jayanthi, *Research Journal of Chemistry and Environment*, **28** (3), 48(2024), <https://doi.org/10.25303/283rjce048055>
6. Kibou, Zahira, Nadia Aissaoui, Ismail Daoud, Julio A. Seijas, María Pilar Vázquez-Tato, Nihel Klouche Khelil, and Nouredine Choukchou-Braham, *Molecules*, **27**(11), 3439(2022), <https://doi.org/10.3390/molecules27113439>

7. Rani, Manviri, and Uma Shanker, *Green Nanomaterial's for Industrial Applications*, 255(2022), <https://doi.org/10.1016/B978-0-12-823296-5.00001-0>
8. A. Kistan, A. Premkumar, V. Kanchana, *Asian Journal of Chemistry*, **34(7)**, 1698(2022) <https://doi.org/10.14233/ajchem.2022.23699>
9. Badawi, Ahmad K., M. Abd Elkodous, and Gomaa AM Ali, *RSC advances*, **11(58)**, 36528(2021), <https://doi.org/10.1039/D1RA06892J>
10. N. Sarvaiya, H. Samata, S. Gulati and H. Patel, *Rasayan Journal of Chemistry*, **15(1)**, 564(2020), <http://dx.doi.org/10.31788/RJC.2022.1516656>
11. R.M. Mohareb, D.H. Fleita and O.K. Sakka, *Molecules*, **23**, 16 (2011), <https://doi.org/10.3390/molecules16010016>
12. Muhammad, Zahir, Farman Ali, Muhammad Sajjad, Nisar Ali, Muhammad Bilal, Mohammed Rafi Shaik, Syed Farooq Adil, Mohammed AF Sharaf, Emad Mahrous Awwad, and Mujeeb Khan, *Catalysts*, **11(1)**, 117(2021), <https://doi.org/10.3390/catal11010117>
13. N.R.Hendekhale, A.Mohammad-Khah, *Journal of Environmental Chemical Engineering*, **8(5)**, 104065 (2020), <https://doi.org/10.1016/j.jece.2020.104065>
14. Momeni, Sarieh, and Ramin Ghorbani-Vaghei, *Scientific Reports*, **13(1)**, 1627(2023), <https://doi.org/10.1038/s41598-023-27940-6>
15. Tavassoli, Amir Mahdi, Mohammad Ali Zolfigol, and Meysam Yarie, *Research on Chemistry Intermediates*, **49(2)**, 679(2023).
16. Manoer, Afaf, and Rehab M. Elbargisy, *Indian Journal of Chemistry-Section B*, **60(9)**, 1272(2021)
17. A. Kistan, V. Kanchana, *Asian Journal of Chemistry*, **35(8)**, 1899(2023) <https://doi.org/10.14233/ajchem.2023.27792>
18. Desai, Nisheeth C., Jahnvi D. Monapara, Aratiba M. Jethawa, and Unnat Pandit, *Recent Developments in the Synthesis and Applications of Pyridines*, 253(2023), <https://doi.org/10.1016/B978-0-323-91221-1.00007-5>
19. O. Mazimba, K. Wale, D. Loeto and T. Kwape, *Bioorganic & Medicinal Chemistry*, **22(23)**, 6564 (2014), <https://doi.org/10.1016/j.bmc.2014.10.015>
20. Nasrollahzadeh, Mahmoud, Nasrin Shafiei, Zahra Nezafat, Nayyereh Sadat Soheili Bidgoli, Fahimeh Soleimani, and Rajender S. Varma, *The Chemical Record*, **20(11)**, 1338(2020), <https://doi.org/10.1002/tcr.202000078>
21. R. Kant, V.K. Gupta, K. Kapoor, M. Sapnakumari, B. Narayana and B.K. Sarojini, *Crystallographic Communications*, **68(10)**, 2917(2012), <https://doi.org/10.1107/S1600536812038202>
22. Liao, Shengliang, Shibin Shang, Minggui Shen, Xiaoping Rao, Hongyan Si, Jie Song, and Zhanqian Song, *Bioorganic & medicinal chemistry letters*, **26(6)**, 1512(2016), <https://doi.org/10.1016/j.bmcl.2016.02.024>
23. EL-Hashash, A. Maher, and Safaa S. Shaban, *Synthetic Communications*, **49(16)**, 630(2019), <https://doi.org/10.1080/00397911.2019.1616096>
24. U. Nisha Mary, D. Venkatesh, S. Arulmurugan, A. Kistan, P. Rajeshwaran, and P. Siva Karthik, *Inorganic Chemistry Communications*, **160**, 111942(2023), <https://doi.org/10.1016/j.inoche.2023.111942>
25. Ismail, Magda MF, Amel M. Farrag, and Asmaa M. El-Nasser, *Polycyclic Aromatic Compounds*, **43(1)**, 630(2023), <https://doi.org/10.1080/10406638.2021.2019800>
26. Hassan, Heba, Mohamed Hisham, Mohamed Osman, and Alaa Hayallah, *Journal of advanced Biomedical and Pharmaceutical Sciences*, **6(1)**, 1(2023), <https://dx.doi.org/10.21608/jabps.2022.162396.1166>
27. Kumar, Nitin, Alka Chauhan, and Sushma Drabu, *Biomedicine & Pharmacotherapy*, **65(5)**, 380(2011), <https://doi.org/10.1016/j.biopha.2011.04.023>
28. Rani, Manviri, Jyoti Yadav, Sudha Chaudhary, and Uma Shanker, *Journal of Environmental Chemical Engineering*, **9(6)**, 106763(2021), <https://doi.org/10.1016/j.jece.2021.106763>

[RJC-8694/2023]